3-4-2013

Insights Into The Roles of Desolvation and π-Electron Interactions During DNA Polymerization

Edward A. Motea
Case Western Reserve University

Irene Lee
Case Western Reserve University

Anthony J. Berdis
Cleveland State University, A.BERDIS@csuohio.edu

Insights into the Roles of Desolvation and n:-Electron Interactions during DNA Polymerization

Edward A. Motea, Irene Lee, and Anthony J. Berdis

This report describes the use of several isosteric non-natural nucleotides as probes to evaluate the roles of nucleobase shape, size, solvation energies, and n-electron interactions as forces influencing key kinetic steps of the DNA polymerization cycle. Results are provided using representative high- and low-fidelity DNA polymerases. Results generated with the f. coli Kienow fragment reveal that this high-fidelity polymerase utilizes hydrophobic nucleotide analogues with higher catalytic efficiencies compared to hydrophilic analogues. These data support a major role for nucleobase desolvation during nucleotide selection and insertion. In contrast, the low-fidelity HIV-1 reverse transcriptase discriminates against hydrophobic analogues and only tolerates non-natural nucleotides that are capable of hydrogen-bonding or n-stacking interactions. Surprisingly, hydrophobic analogues that function as efficient substrates for the £ *coli* Kienow fragment behave as noncompetitive or uncompetitive inhibitors against HIV-1 reverse transcriptase. In these cases, the mode of inhibition depends upon the absence or presence of a templating nucleobase. Molecular modeling studies suggest that these analogues bind to the active site of reverse transcriptase as well as to a nearby hydrophobic binding pocket. Collectively, the studies using these non-natural nucleotides reveal important mechanistic differences between representative high- and low-fidelity DNA polymerases during nucleotide selection and incorporation.

Introduction

DNA polymerases catalyze the addition of mononucleotides into a growing polymer (primer), typically using a DNA template as a guide to direct each incorporation event. The chemical mechanism for DNA polymerization is simple nucleophilic attack by the 3'-0H of the primer on the a-phosphate of the incoming dNTP. Although the chemical mechanism of this reaction is well defined,11[1] there still remain many questions regarding the molecular details of kinetic steps that precede the phosphoryl transfer step. For example, how do polymerases accurately read a DNA template strand to decide which of the four natural dNTPs should be correctly incorporated into the growing primer? This is an important question as DNA is heteropolymeric, and the changing nature of the templating strand places additional strains on the unusually high demand for substrate specificity to maintain genomic fidelity. Paradoxically, polymerases must be highly selective to insert only one of four potential dNTPs opposite a templating nucleobase while also being extraordinarily flexible to recognize distinct pairing partners. Furthermore, a polymerase must perform the repetitive task of nucleobase pairing and phosphodiester bond formation with incredible speed.£2[1]

Several models, including positive/negative selection.r3[1] thermodynamic stability}[41] and steric constraints/shape complementarity,15[1] have been proposed to account for how polymerases maintain fidelity during DNA synthesis. While each model invokes distinctive features, they all argue that the functional groups present on the nucleobases are important for efficient polymerization. Indeed, these functional groups regulate polymerization efficiency and fidelity by consummating proper hydrogen-bonding interactions between the incoming nucleotide and the templating nucleobase. However, the reliance on hydrogen-bonding as the sole factor influencing efficient DNA synthesis has been challenged by the demonstration that non-natural nucleotides lacking classical hydrogen-bonding groups are viable polymerase substrates.161 Perhaps the most-cited example of this observation is the demonstration that 2,4-difluorotoluene, an isosteric analogue of dTIP, is enzymatically incorporated opposite a templating adenine with remarkably high efficiency.16a1 While these studies provide compelling evidence that DNA polymerization can indeed occur in the absence of hydrogen-bonding potential, there still remain several questions regarding how other biophysical features such as shape/size, nucleobase hydrophobicity, and n-electron interactions are used during polymerization.

To more accurately examine these features, we developed a series of 5-substituted indolyl-2'-deoxynucleotides as mechanistic probes for the replication of normal DNA in addition to several distinct DNA lesions.[7) For example, the isosteric non-natural nucleotides illustrated in Figure 1A were employed to study how the high-fidelity bacteriophage T4 DNA polymerase uses nucleobase hydrophobicity and n-electron interactions

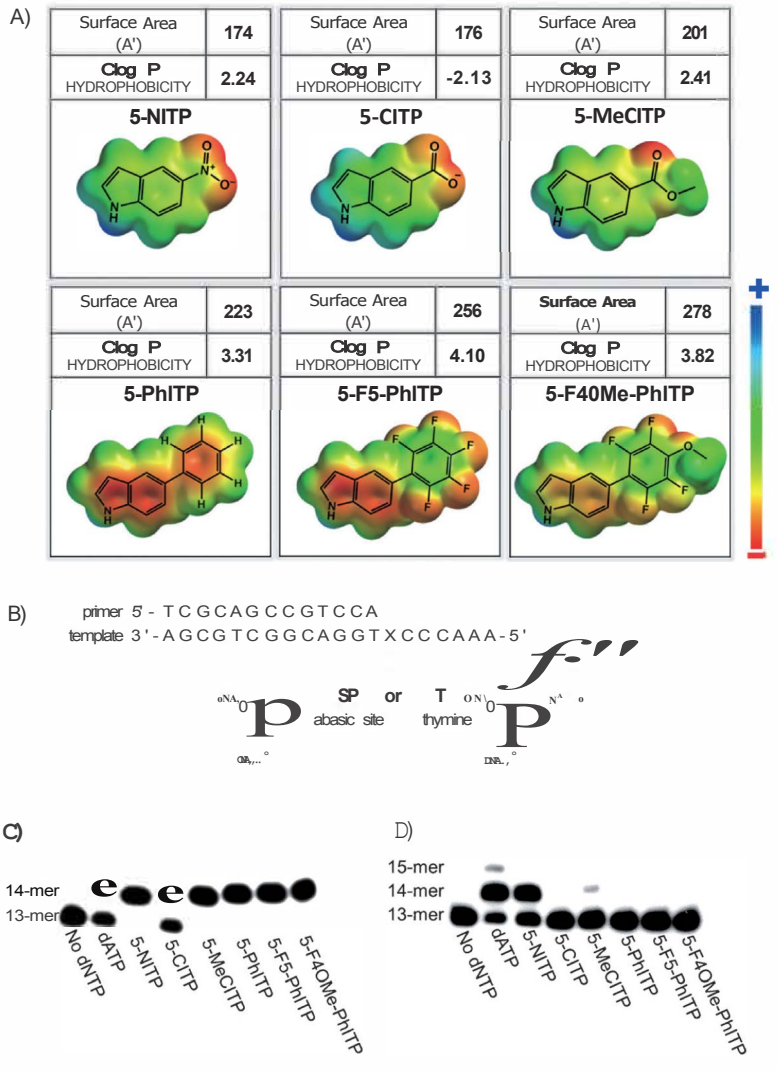

Figure 1. A) Chemical structure and physicochemical properties of non natural nucleo tides used in this study. For clarity, only the nucleobases are shown. Surface areas (used as an indicator of the relative size of the nucleobase), Clog *P* and electrostatic density po tential map shown for each nucleobase were calculated using the Spartan '08 software. The semi empirical method of calculation with AM1 was used for geometry optimization and the density functional theory level of calculation with B3LYP 6 31 G** basis sets were used for energy minimization. B) DNA substrate sequence used in this study. C) The in corporation of natural (dATP) and various non natural nucleotides opposite an abasic site catalyzed by the *E.coli* Kienow fragment. Aliquots of the reaction were quenched using EDTA (200 mM). The total reaction time was 5 min. D) The utilization of natural (dATP) and various non natural nucleotides opposite an abasic site catalyzed by HIV 1 RT. Ali quots of the reaction were quenched using EDTA (200 mM). The total reaction time was 60 min. See text for complete details regarding experimental conditions.

during the replication of normal DNA and an abasic site, a non-instructional DNA lesion.[81] The first class of analogues (5-NITP, 5-CITP, and 5-MeCITP) were used to quantify the role of nucleobase hydrophobicity and desolvation. The second class (5-PhITP, 5-FS-PhITP, and 5-F40Me-PhITP) were used to evaluate the importance of n-electron density and size variation. Collectively, this study demonstrated that the catalytic efficiency, $k_{pol}/K_{d,app}$ for incorporating these non-natural nucleotides is governed by their intrinsic hydrophobicity and degree of Jt-electron density_[81] This information was used to propose a model in which the binding affinity of the nucleotide is controlled by nucleobase desolvation while n-electron density facilitates the conformational change step preceding phosphoryl transfer.

It should be noted that this previous study employed the bacteriophage T4 DNA polymerase, a prototypical family B member of DNA polymerases that is recognized for its remarkable high fidelity when replicating undamaged DNA.[9l This report attempts to extend these findings by quantifying the ability of different DNA polymerases, the *E coli* Kienow fragment (family A) and HIV-1 reverse transcriptase (family RT), to utilize these non-natural nucleotides when replicating normal DNA or an abasic site. The goal is to determine if nucleobase desolvation and Jt-electron interactions play similar roles with these other DNA polymerases. Indeed, the results presented here indicate that DNA polymerization does not occur through a "universal" mechanism. Instead, DNA polymerases utilize distinct biophysical features when replicating normal and damaged forms of DNA. This is evident as the f. *coli* Kienow fragment and HIV-1 RT show unique behavior when utilizing these different classes of isosteric non-natural nucleotides. In general, HIV-1 RT shows higher discrimination against incorporating non-natural nucleotide analogues opposite an abasic site or templating DNA compared to the Kienow fragment. This dichotomy can be explained by significant differences in the composition and architecture of the active sites of each DNA polymerase. In addition, these non-natural nucleotides display unique inhibitory effects against HIV-1 RT. Collectively, this information provides new insights into the mechanism of DNA polymerization as well as applications towards developing novel inhibitors against viral DNA polymerases.

Results

HIV-1 RT and f. *coli* Kienow fragment replicate an abasic site through distinct mechanisms

Our studies begin by using the isosteric non-natural nucleotides shown in Figure 1A to quantify the contributions of shape, size, nucleobase desolvation, and n-electron interactions when replicating an abasic site. We focused on this lesion as the lack of coding information minimizes the influence of direct hydrogen-bonding interactions during kinetic steps encompassing nucleotide binding, conformational changes, and phosphoryl transfer. In addition, the use of 5-substituted indolyl-2'-deoxynucleotides is an important way of quantifying the influence of the aforementioned biophysical features. For example, analogues such as 5-NITP, 5-CITP, and 5-MeCITP are nearly identical with respect to overall shape/size and n-electron density (Figure 1A and Table 51 in the Supporting Information). However, since 5-CITP is far more hydrophilic than 5-NITP and 5-MeCITP, variations in its utilization can be attributed to differences associated with nucleobase hydrophobicity. Similar arguments

Table 1. Summary of kinetic parameters for the incorporation of natural and non natural nucleotides opposite an abasic site catalyzed by the *E.coli* Kienow fragment[a] or HIV 1 RT[b].

Polymerase	Analogue	K_m [μM]	k_{ca}, [s 1]	k_{ca}/K_m [M 1s ']
KF	dATP	34±6	0.18±0.01	5290
KF	5 NITP	8±2	0.24±0.02	30000
KF	5 CITP	125±30	0.40±0.03	3200
KF	5 MeCITP	5.4±0.7	0.6±0.1	111 000
KF	5 PhlTP	14.3±0.3	0.42±0.04	29400
KF	5 FS PhlTP	3.0±0.4	0.40±0.01	133300
KF	5 F40Me PhlTP	2.6±0.4	0.61 ±0.03	234600
RT	dATP	70±13	0.0093 ± 0.0008	133
RT	5 NITP	58±18	0.0084 ± 0.0006	145
RT	5 CITP	n.d.lcl	n.d.	n.d.
RT	5 MeCITP	106±35	0.0058 ± 0.0002	55
RT	5 PhlTP	n.d.	n.d.	n.d.
RT	5 FS PhlTP	n.d.	n.d.	n.d.
RT	5 F40Me PhlTP	n.d.	n.d.	n.d.

[al Assays were performed using Kienow fragment (12 nM) and DNA substrate (1000 nM) with variable nucleotide concentrations (0 500 μM). [bl Assays were performed using of HIV 1 reverse transcriptase (SO nM) and DNA substrates (500 nM) with variable nucleotide concentrations (0 500 μM). [cl Not determined as incorporation was too low to measure accurately even at the highest nucleotide concentration used (500 μM). n.d.: not determined.

can be made using 5-PhlTP and the fluorinated analogues, 5-F5-PhlTP and 5-F40me-PhlTP, to evaluate the roles of :rt-electron interactions.

The ability of Kienow fragment and HIV-1 RT to incorporate nucleotides opposite an abasic site was tested using the DNA substrate depicted in Figure 1B. Denaturing gel electrophoresis images provided in Figure 1C and D show that dATP is utilized by both DNA polymerases, and this result is consistent with previous reports_!,oJ Despite this similarity, however, the two polymerases differ in their ability to utilize the non-natural nucleotides examined here. For example, the Kienow fragment incorporates all six non-natural nucleotides opposite the non-instructional abasic site while HIV-1 RT only incorporates two of the six analogues (5-NITP and 5-MeCITP). This later result is surprising since HIV-1 RT typically displays low fidelity and was thus predicted to utilize all of these non-natural nucleotides, especially 5-PhlTP which has enhanced base-stacking properties[Y 1]

To further assess this dichotomy, k,av K_m, and k_{cat}/K_m values for these non-natural nucleotides were measured using both DNA polymerases. These parameters, summarized in Table 1, indicate that the E.coli Kienow fragment and HIV-1 RT differ mechanistically as they rely on different biophysical features to select and incorporate nucleotides opposite an abasic site. In the sections below, the distinctive features of each DNA polymerase are discussed regarding their ability to utilize or discriminate against these novel non-natural nucleotides.

The importance of nucleobase desolvation with the *E coli* Kienow fragment

At face value, the data appear to support a model invoking steric constraints/shape complementarity as the overall catalytic efficiencies (k_{cat}/K_m) for nucleotide utilization correlates with the size and shape of the non-natural nucleotide. For example, k_{cat}/K_m values increase from the lowest value of 3200 $M^{-1}s^{-1}$ for the small analogue, 5-CITP, to the highest value of 235000M-1s_, measured with the largest analogue, 5-F40Me-PhlTP. This result is consistent with previous reports indicating that large analogues such as 5-cyclohexyl-2'-deoxynucleoside triphosphate (5-CHITP) are utilized with higher efficiencies compared to smaller analogues such as indolyl-2'-deoxynucleoside triphosphate (IndTP).!10aJ[1]

However, closer inspection of the individual k_{cat} and K_m parameters do not support a steric fit model as there is not a clear correlation between the shape/size of a non-natural nucleotide with its K_m value. Instead, the hydrophobicity of the non-natural nucleobase appears to play a large role in influencing K_m. This is evident as the K_m value of 8 μM for the hydrophobic analogue, 5-NITP, is significantly lower than the K_m value of 125 μM measured for the hydrophilic analogue, 5-CITP. In this case, the 16-fold higher K_m value for 5-CITP must reflect differences in nucleobase hydrophobicity since both analogues are essentially identical with respect to size, shape, and :rt-electron density. This mechanism is further supported as the K_m value for the other hydrophobic analogue, 5-MeCITP, is - 25-fold lower than its hydrophilic counterpart, 5-CITP (compare 5.4 μM versus 125 μM, respectively). Similar observations were reported with the high-fidelity bacteriophage T4 DNA polymerase/[8]l and this commonality suggests that nucleobase hydrophobicity plays a vital role in the binding affinity of the incoming nucleotide with members of the A and B families of DNA polymerases.

This mechanism was further investigated by comparing the kinetic parameters for the isosteric analogues, 5-PhlTP, 5-F5-PhlTP, and 5-F40Me-PhlTP. These analogues are similar in shape and size but differ with respect to the degree of :rt-electron density. Previous studies with the bacteriophage T4 DNA polymerase showed that the :rt-electron-rich nucleotide, 5-PhlTP, was utilized as efficiently as the :rt-electron-deficient analogues, 5-F5-PhlTP and 5-F40Me-PhlTP.!8l With the Kienow fragment, however, both 5-F5-PhlTP and 5-F40Me-PhlTP display higher k_{cat}/K_m values compared to 5-PhlTP. Rather than influencing k_{cat}• these fluorinated analogues have lower K_m values compared to 5-PhlTP (compare 3.0 μM for 5-F5-PhlTP and 2.6 μM for 5-F40Me-PhlTP versus 14.3 μM for 5-PhlTP). Since these fluorinated nucleotides are more hydrophobic than their

Table 2. Summary of kinetic parameters for the incorporation of natural and non natural nucleotides opposite a thymine template catalyzed by the Kienow fragment[a] or HIV 1 reverse transcriptase[b].

Polymerase	Analogue	K_m [µM)]	k_{cat} [s^{-1}]	k_{cat}/K_m [M^{-1}s^{-1}]
KF	dATP'	5±1	50±5	10000000
KF	5 NITP	34±8	0.0042 ± 0.0002	120
KF	5 CITP	nd_ld	n.d.	n.d.
KF	5 MeCITP	50±13	0.007 ± 0.001	140
KF	5 PhlTP	21 ± 4	0.005 ± 0.001	240
KF	5 FS PhlTP	94±22	0.011 ±0.001	120
KF	5 F40Me PhlTP	24±5	0.01 0± 0.001	420
RT	dATP	0.41 ±0.07	0.084 ± 0.004	205000
RT	5 NITP	n.d.	n.d.	n.d.
RT	5 CITP	n.d.	n.d.	n.d.
RT	5 MeCITP	n.d.	n.d.	n.d.
RT	5 PhlTP	n.d.	n.d.	n.d.
RT	5 FS PhlTP	n.d.	n.d.	n.d.
RT	5 F40Me PhlTP	n.d.	n.d.	n.d.

[a] Assays were performed using Kienow fragment (60 nM) and DNA substrate (1000 nM) with variable nucleotide concentrations (0 500 µM). [bl Assays were performed using HIV 1 reverse transcriptase (SO nM) and DNA substrates (500 nM) with variable nucleotide concentrations (0 500 µM). [cl Kinetic values taken from [1 OJ. [d] Not determined as the amount of nucleotide incorporation was too low to measure accurately even at the highest nucleotide concentration tested (500 µM). n.d.: not determined.

nonfluorinated counterpart,l1 2l their lower K_m values again support an important role for nucleobase desolvation as a key determinant for efficient nucleotide incorporation opposite an abasic site.

The k_{cat}, K_m, and k_{cat}/K_m values for these isosteric non-natural nucleotides were also measured for incorporation opposite a templating thymine. As summarized in Table 2, the presence of thymine markedly reduces their catalytic efficiencies. This occurs as both the k_{cat} and K_m values are adversely influenced, and these effects are consistent with models invoking steric fit and shape complementarity as important features for normal DNA replication_[sJ In general, these data argue that steric fit/shape complementarity play important roles for nucleotide selection by the *E coli* Kienow fragment during normal DNA synthesis. However, nucleobase hydrophobicity plays a larger role during the replication of non-instructional DNA lesions such as an abasic site.

HIV-1 RT requires enthalpic interactions for nucleotide incorporation

Identical kinetic analyses were performed using HIV-1 RT, a low-fidelity DNA polymerase, to quantify the incorporation of these isosteric analogues opposite normal and damaged DNA. The data summarized in Table 1 highlight several important mechanistic differences between HIV-1 RT and the *E.coli* Kienow fragment. As described earlier, HIV-1 RT utilizes only two non-natural nucleotides, 5-NITP and 5-MeCITP, during the replication of an abasic site. In addition, both analogues display low catalytic efficiencies that are essentially identical to the natural substrate, dATP. These results contrast those obtained with the Kienow fragment which displays higher catalytic activity with these non-natural nucleotides. Finally, HIV-1 RT does not utilize large, hydrophobic analogues (5-PhlTP, 5-FS-PhlTP, and 5-F40Me-PhlTP), and again contrast results obtained with the Kienow fragment.

Non-natural nucleotides are unique HIV-1 RT inhibitors

The inability of HIV-1 RT to incorporate non-natural nucleotides could result from a lack of nucleotide binding or by an inability of these analogues, once bound to the Pol-DNA complex, to induce a conformational change necessary for phosphoryl transfer. These possibilities were examined by testing the inhibitory effects of these analogues against HIV-1 RT during the replication of an abasic site or normal DNA. The data provided in Figure 2A shows that dAMP incorporation opposite an abasic site is progressively inhibited with increasing concentrations of 5-CITP. Dixon plot analysis yields an apparent K_i value of (19 ± 4) µM for 5-CITP (Figure 2 B), and correction for the concentration of the natural substrate using the Cheng-Prusoff equation [13J yields a true K_i value of (8.1 ±1.7) µM. Similar analyses yield a K_i value of (7.9± 2.4) µM for 5-PhlTP opposite the abasic site (Table 3). In general, the inhibitory effects produced by these non-natural nucleo-

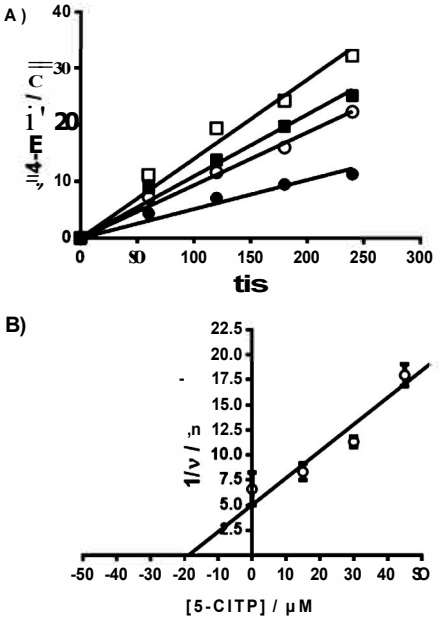

Figure 2. Inhibition of HIV 1 RT activity by 5 CITP. A) Representative time courses for the incorporation of dATP opposite an abasic site in the absence and presence of varying 5 CITP inhibitor concentrations. The concentration of 5 CITP is denoted by the following: 0 µM (o), 15 µM (•), 30 µM (o), and 45 µM (el nucleotide. B) Dixon plot analysis yields an apparent K_i of 19 µM. The true K_i value of (8.1 ± 1.7) µM was obtained using the Cheng Prusoff equation.

Table 3. Summary of inhibition constants and mode of inhibition for non natural nucleotides against HIV 1 RT transcriptase during translesion and correct DNA synthesis.

Template	Inhibitor	K_i [µM]	Mode of inhibition	K_m [µM]	K_{ii} [µM]
abasic site	5 CITP	8.1 ±1.7			
abasic site	5 CITP		competitive	11.0±1.1	n.a.
abasic site	5 PhITP	7.9±2.4			
abasic site	5 PhITP		noncompetitive	20.1 ±1.2	30.6±1.1
thymine	5 CITP	44±14			
thymine	5 CITP		competitive	18.8±0.3	n.a.
thymine	5 PhITP	32±7			
thymine	5 PhITP		uncompetitive	n.a.	27.0± 1.6
thymine	5 NITP	26± 11			
thymine	5 MeCITP	86±13			

n.a.: not applicable.

tides validate that they bind to HIV-1 RT but are unable to interact productively for catalysis. However, the identity in the inhibition constants for 5-CITP and 5-PhITP is surprising as these analogues differ significantly with respect to shape, size, and nucleobase hydrophobicity.

The inhibition constants for 5-CITP, 5-PhITP, 5-NITP, and 5-MeCITP were next measured during the replication of thymine to further elucidate the mechanism of nucleotide binding. As expected, each analogue inhibits dAMP incorporation (Table 3). In addition, the K_i values measured opposite a templating base are ~fivefold higher than those measured opposite the non-templating abasic site. The difference in potency could reflect simple steric hindrance as the presence of the templating base is expected to hinder binding of the non-natural nucleotide. Unfortunately, this simple explanation is incomplete as the measured K_i values do not correlate with the size and/or shape of the corresponding non-natural nucleotides. For example, the K_i values for 5-CITP and 5-MeCITP, which are predicted to be adequate pairing partners for thymine, are higher than that measured for 5-PhITP, a larger analogue that should not properly pair with thymine.

Double reciprocal plot analyses were next performed to define the mode of inhibition for several of these nucleotide analogues. Representative data provided in Figure 3A shows that the hydrophilic nucleotide, 5-CITP, behaves as a competitive inhibitor versus dATP when replicating an abasic site. This analysis yields a K_i value of (11.0 ± 1.1) µM which is in excellent agreement with the K_i value of (8.1 ± 1.7) µM measured above using Dixon plot analysis (vide supra). Likewise, 5-CITP acts as a competitive inhibitor versus dATP during normal DNA synthesis, displaying a higher K_i of (18.8 ± 0.3) µM.

Similar analyses performed with 5-PhITP show that this non-natural nucleotide behaves as a noncompetitive inhibitor versus dATP during the replication of an abasic site (Figure 3C).

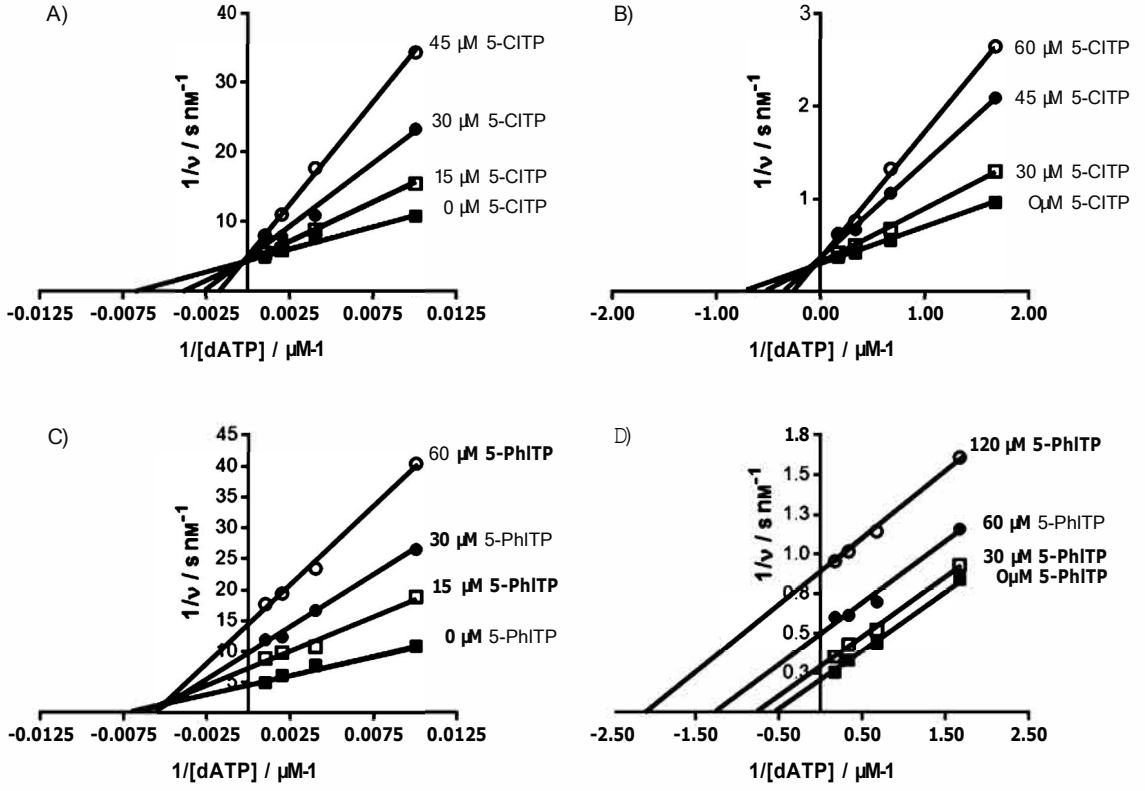

Figure 3. Double reciprocal plot analyses used to define the mode of inhibition by 5 CITP and 5 PhITP against HIV 1 RT. dATP incorporation opposite an abasic site or a thymine template. A) 5 CITP acts as a competitive inhibitor against dATP incorporation opposite an abasic site (DNA_5,). B) 5 CITP acts as a competitive inhibitor against dATP incorporation opposite a templating thymine (DNAr). C) 5 PhITP acts as a noncompetitive inhibitor against dATP incorporation opposite an abasic site. D) 5 PhITP acts as an uncompetitive inhibitor against dATP incorporation opposite a templating thymine (DNAr).

This contrasts the competitive inhibition observed with 5-CITP and indicates that 5-PhITP binds to two different sites on the polymerase.[141] Fits of the data to Equation (6) provide a K_i value of (20.1 ± 1.2) μM which likely corresponds to the binding of 5-PhITP to the RT-DNAsp binary complex and a K_i value of (30.6 ± 1.1) μM which represents 5-PhITP binding to a different enzyme form, most likely the RT-DNAsp-dATP ternary complex. This model was validated by defining the mode of inhibition during the replication of undamaged DNA. As illustrated in Figure 3 D, the inhibition pattern of 5-PhITP changes from non-competitive during the replication of an abasic site to uncompetitive during the replication of undamaged DNA. In this case, the K_i value of (27.0 ± 1.6) μM is nearly identical to the K_i value of (30.6 ± 1.1) μM measured using DNA containing an abasic site, and this suggests that 5-PhITP inhibits the retroviral polymerase by binding to a potential allosteric site.

Molecular modeling studies

The dichotomy in nucleotide utilization between these DNA polymerases was explored using existing structural information[151] to compare the amino acid composition and architecture of their active sites within 5 A of the primer-template junction. As illustrated in Figure 4 A, the active site of the Kienow fragment contains two aromatic amino acids, F762 and Y766, that lie approximately 4 A away from the primer terminus. Figure 4 B shows that the same region of HIV-1 RT is considerably different as R72 and Ql 51 occupy sites that are equivalent to F762 and Y766, respectively, in the Kienow fragment. Although these polar and hydrophilic amino acids have been implicated in stabilizing the transition state during phosphoryl transfer/[161] our analysis here suggests a potential role in nucleotide selection and/or conformational changes associated with polymerization.

Discussion

Hydrogen-bonding, steric constraints, nucleobase hydrophobicity, desolvation energies, n-n stacking, and n-cation stacking interactions play important roles in defining the double helical nature of DNA. However, quantifying their contributions during various enzymatic processes such as DNA replication and DNA repair has proven to be difficult. Much of this difficulty arises from the intrinsic properties of natural nucleotides as they typically possess differing "amounts" of each biophysical feature. For example, guanine possesses a larger surface area than adenine and has more functional groups capable of hydrogen-bonding interactions. However, adenine has better base-stacking capabilities compared to guanine due to its more aromatic and hydrophobic nature. These differences make it difficult to unambiguously define the roles of these features. To combat these complications, recent efforts have focused on using non-natural nucleotides, that is, nucleotide analogues with non-hydrogen bonding groups, as artificial substrates to more accurately define the influence of these features during DNA polymerization. The strategy of this approach is to selectively introduce diverse functional groups at a defined position of a simple molecular scaffold that mimics a purine or pyrimidine.[16a-gl a-d] For example, we recently developed two classes of isosteric non-natural nucleotides to probe the mechanism of polymerization catalyzed by the high-fidelity bacteriophage T4 DNA polymerase.[18] These studies demonstrated that the initial binding step of the non-natural nucleotide is governed by energies involving nucleobase desolvation while the conformational change step preceding phosphoryl transfer is controlled by a combination of nucleobase hydrophobicity and n-electron density. In the present study, we investigated if this model can be accurately applied to other DNA polymerases such as HIV-1 RT and the E. *coli* Kienow fragment. The results here indicate that a "universal" mechanism does not exist, at least in the context of using 5-substituted-indolyl-2'-deoxynucleotides. In fact, the use of these non-natural analogues provides some unexpected results that illustrate the molecular diversity used by each enzyme to achieve efficient DNA polymerization. For instance, it is surprising that the "error-prone" HIV-1 RT shows a remarkable ability to discriminate against using nucleotide analogues that lack canonical hydrogen-bonding groups. These results differ from those re-

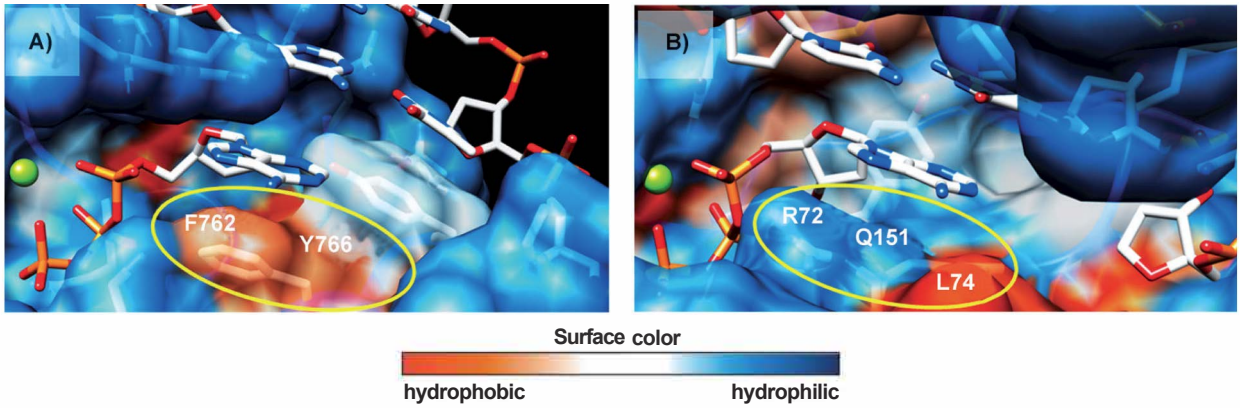

Figure 4. Kyte Doolittle hydrophobicity surface structural models for A) Kienow fragment and B) HIV 1 RT. These models were generated using UCSF Chimera 1.5.3. The abasic site was created through PyMol builder from the crystal structure of the ternary complex HIV 1 RT DNA dATP (PDB ID: 3KK2). The putative ternary complex of the Kienow fragment was modeled from the crystal structure of KlenTaq polymerase (PDB ID 3LWL) using the Molecular Operating Environment (MOE 2010.10) package as described in the Experimental Section.

ported by Kool's group who demonstrated that HIV-1 RT can efficiently incorporate several nonpolar isosteric analogues of dTIPY [7] The reason for this kinetic difference is currently unknown. However, one possibility could reflect intrinsic differences between using small, non-natural analogues such as disubstituted toluene derivatives versus larger 5-substituted-indolyl-2'-deoxynucleotides. Another difference could reflect the influence of functional groups that are more chemically diverse (NO_2, CO_2, and $COOCH_3$) compared to simple halogens (F, Cl, and Br). While these differences warrant further investigations, the inability of HIV-1 RT to utilize our 5-substituted indolyl-2'-deoxynucleotides is particularly interesting as the Kienow fragment, a polymerase with higher intrinsic fidelity, incorporates these hydrophobic non-natural nucleotides opposite a templating thymine (Table 2).

The kinetic preference of the *E coli* Kienow fragment to use non-natural nucleotides during the replication of an abasic site appears very similar to that for the high-fidelity bacteriophage T4 DNA polymerase. In fact, both polymerases preferentially utilize non-natural nucleotides that have strong base-stacking properties, i.e., analogues that are hydrophobic and rich in n-electron density. This is evident as the Kienow fragment and T4 DNA polymerase both incorporate 5-NITP opposite an abasic site much more efficiently than the preferred natural nucleotide, dATP [10•, isi However, comparison of structural data from the Thermus aquaticus KlenTaq polymerase [19] and the bacteriophage RB69 DNA polymerase [20] reveal different interactions of 5-NITP within the active site of either enzyme, The structure of the RB69 DNA polymerase bound to an abasic-site containing DNA and 5-NITP shows that the non-natural nucleotide exists in an intrahelical position. In this conformation, the nitro moiety extends into the void of the abasic site such that the non-natural nucleobase stacks under the template strand. This structural data indicates that steric constraints do not play a significant role in nucleotide selection. Instead, nucleobase hydrophobicity and n-n interactions of the nitroindole moiety with the penultimate base pair play the predominant roles. Furthermore, when paired opposite an abasic site, the indole ring of the non-natural nucleotides is superimposable with the adenine ring of dATP when it is present in a Watson-Crick base pair with thymine, Thus, the RB69 polymerase structure shows that 5-NITP adopts a "normal" conformation in DNA, even when incorporated opposite a nontemplating abasic site.

Results obtained with the *T* aquaticus KlenTaq polymerase offer a different interpretation for the enhanced incorporation kinetics for 5-NITP opposite the lesion. [19] In this case, the interaction of natural nucleotides including dATP, dGTP, and dTIP with the active-site amino acid, Y671, plays an intricate role in governing nucleotide selection during the replication of an abasic site. In fact, these interactions appear to regulate the distance between the alpha phosphate of the incoming nucleotide with the 3'-hydroxyl of the primer template. Thus, this type of steric fit mechanism ultimately influences the rate for the incorporation of these natural nucleotides opposite the lesion, However, this steric fit mechanism does not appear to be operational with 5-NITP as the non-natural nucleotide does not interact with Y671. Instead, the enhanced base-stacking properties of 5-NITP "bypass" the normal steric fit mechanism favored by KlenTaq_il [9] As a consequence, the higher catalytic efficiency for 5-NITP during translesion DNA synthesis is thought to represent a noncanonical pathway compared to natural dNTPsY [9]

We acknowledge that the kinetic data presented here cannot provide additional insight into the interactions of non-natural nucleotides with Y671. However, these data can provide important insight into molecular mechanisms for the recognition of non-natural nucleotides. In this case, molecular models of existing polymerase structures were used to compare and contrast the potential interactions of non-natural nucleotides with specific amino acids in the active sites of the *E coli* Kienow fragment and HIV-1 RT. The active site of the Kienow fragment contains two aromatic amino acids, F762 and Y766, that lie approximately 4 A away from the primer terminus (Figure 4A). We argue that these particular amino acids create an energetically favorable environment that facilitates the binding of hydrophobic non-natural nucleotides such as 5-NITP and 5-MeCITP. Likewise, these hydrophobic amino acids would negatively affect the binding of hydrophilic analogues, This is most evident as the catalytic efficiency of 3200 M-1 s-1 measured with the hydrophilic 5-CITP is approximately ten times lower than the hydrophobic isostere, 5-NITP (30000 M-1 s-1). This difference, corresponding to a $t.t.G$ value of 1.33 kcal mo1-1, likely reflects the energetic contributions of nucleobase desolvation during the initial binding step. Similar results were obtained with the bacteriophage T4 DNA polymerase during the replication of an abasic site as the energetic contribution of nucleobase desolvation was greater during ground state binding ($t.t.G$ = 1.3 kcal mol-1) compared to the rate constant for incorporation ($t.t.G$ = 0.4 kcal mol-1).18

In HIV-1 RT, R72 and Q151 occupy sites that are equivalent to F762 and Y766, respectively, in the Kienow fragment The physical differences in these amino acids can partially explain the dichotomy in nucleotide selection and utilization between either DNA polymerase. For example, the inhibitory effects of the hydrophilic analogue, 5-CITP, could be caused by favorable interactions with R72 and Q151 which are both polar and hydrophilic. While 5-CITP binds to HIV-1 RT with reasonably high affinity (K_i < 10 μM), its inability to be incorporated suggests that these interactions with 5-CITP result in a nonproductive conformation that prevents phosphoryl transfer. Surprisingly, both 5-MeCITP and 5-NITP are incorporated opposite an abasic site, albeit with low catalytic efficiencies. The utilization of 5-MeCITP could reflect favorable hydrogen-bonding interactions of its carbonyl moiety with the polar side chains of either amino acid, While the nitro moiety of 5-NITP does not participate in classical hydrogen bonding interactions, it could engage in dipole-induced interactions with DNA bases and/or polar amino acids that reside in the active site of HIV-1 RT, Further studies are required to more accurately evaluate this possibility.

Another unique feature of this study is that hydrophobic nucleotides such as 5-PhlTP can bind to multiple sites on HIV-1 RT. Specifically, the noncompetitive inhibition displayed by 5-PhlTP indicates that this hydrophobic analogue binds to the

polymerase's active site as well as to a potential allosteric site. The structural model provided in Figure 5A highlights potential binding interactions of 5-PhITP within a hydrophobic pocket that lies adjacent to the active site. This hydrophobic

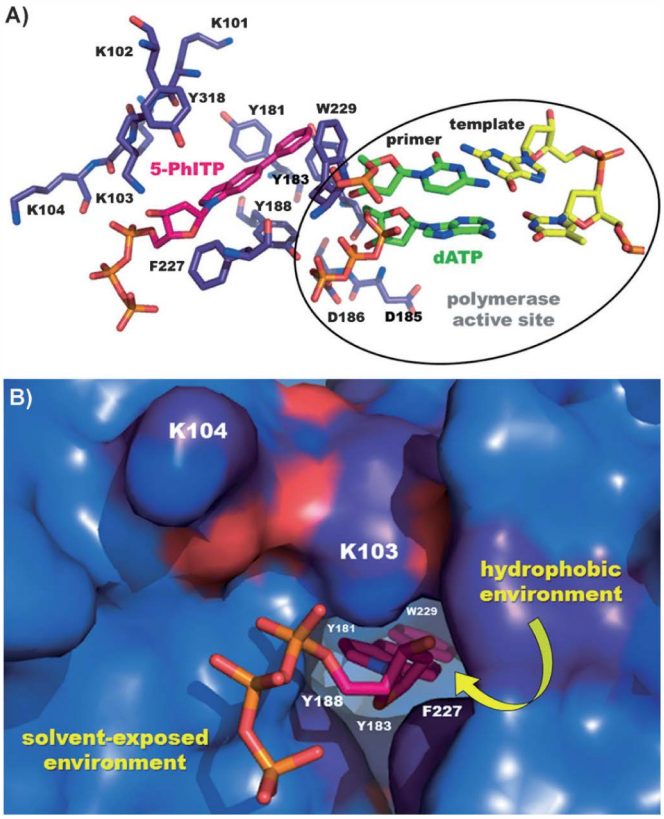

Figure 5. Putative three dimensional structure of HIV 1 RT. A) Structural model of HIV 1 RT in complexed with 5 PhITP (CPK stick representation with carbon atoms in magenta) docked in a hydrophobic allosteric site (key residues are shown in CPK stick representation with carbon atoms in purple color) adjacent to the polymerase active site. B) Surface representation of HIV 1 RT model highlighting the putative positioning of 5 PhITP (CPK stick representation with carbon atoms in magenta) with respect to key residues of the allosteric binding pocket. These models were generated using the PyMol Modeling software by first aligning the primary amino acid sequences of 1HMI (HIV 1 RT DNA binary complex) and 3Q09 (HIV 1 RT NNRTI binary complex) as further described in the Experimental Section.

pocket was originally identified as the binding site for non-nucleoside reverse transcriptase inhibitors (NNRTIs) including Nevirapine and EfavirenzY[11] NNRTIs do not resemble nucleoside analogues and thus function as uncompetitive inhibitors by binding to the RT-DNA-dNTP complex as opposed to free RT or RT-DNA complexY[21] Furthermore, NNRTIs bind to a pocket that lies -1 OA from the polymerase's active site and that is lined with large and hydrophobic amino acids including Yl 81, Y188, F227, and L234.[1231] Our modeling studies suggest that the 5-phenylindole moiety of 5-PhITP could also bind in this region (Figure 5A and B). In this model, favorable :rt-:rt stacking and hydrophobic interactions could be made between the 5-phenylindole moiety with several of aromatic residues (Yl 81, Y183, Y188, F227, and W229). The binding of 5-PhITP could also be assisted through electrostatic interactions that exist between the triphosphate group with one or more lysine residues (K101-K104) that lie within 6-10 A from this hydrophobic pocket. In support of this mechanism, the potency of 5-PhIDP, the diphosphate form of the non-natural nucleotide, is reduced twofold compared to the triphosphate, 5-PhITP (Figure 52). We note, however, that additional studies such as structural characterizations are needed to firmly establish the binding of 5-PhITP at this site.

The identification of a non-natural nucleotide that interacts with both catalytic and allosteric sites of HIV-1 RT could have important implications for developing new therapeutic agents against this viral polymerase. For example, nucleoside-based inhibitors such as AZT and ddC are often combined with NNRTIs in order to synergistically reduce viral loads in patients infected with HIV. Combining both drugs produces additional benefits by delaying the onset of drug resistance caused by pyrophosphorolytic removal of conventional chain-terminating nucleotidesY[41] While therapeutically effective, the use of multiple drug regimens can produce various complications including potential toxicity due to adverse drug-drug interactions_l[2]s[1] The studies here show that 5-PhITP can function as a single chemical entity to inhibit HIV-1 RT through multiple mechanisms. In this respect, the uncompetitive inhibition displayed by 5-PhITP is preferred over conventional inhibitors that work in a competitive manner. This preference reflects the difficulty in achieving drug resistance against an uncompetitive inhibitor since increasing substrate concentrations cannot relieve the inhibitory effects of the compound that is commonly observed with competitive inhibitors. In addition, the use of a single entity to synergistically inhibit HIV-1 RT can reduce complications arising from pharmacodynamic and pharmacokinetic variables associated with different drugs. The ability of the corresponding non-natural nucleoside to function as an anti-viral agent is currently being investigated.

Conclusions

Using several different non-natural nucleotides, we were able to demonstrate that high- and low-fidelity DNA polymerases utilize distinct molecular features for nucleotide recognition and incorporation. In particular, HIV-1 RT appears to utilize 5-substituted indolyl-nucleotides that are capable of hydrogen-bonding interactions whereas the high-fidelity Kienow fragment preferentially utilizes hydrophobic analogues rather than those that are hydrophilic. Finally, several of the hydrophobic analogues display unique inhibitory effects against HIV-1 RT, a feature that might be exploited for therapeutic intervention.

Experimental Section

Materials: [y-32P]ATP was purchased from PerkinElmer Life Sciences. All oligonucleotides, including those containing a tetrahydrofuran moiety mimicking an abasic site, were synthesized by Operon Technologies (Alameda, CA). Oligonucleotides were purified as previously described[17] using denaturing polyacrylamide gel electrophoresis for single-strand DNA and native polyacrylamide gel electrophoresis for duplex DNA. HIV-1 reverse transcriptase was purchased from Calbiochem (San Diego, CA). The Kienow fragment

of DNA polymerase I from E *coli* was purified and quantified as described.[26] All non-natural nucleotides were synthesized and characterized as previously described.[18] All other materials were obtained from commercial sources and were of the highest quality available.

Measurements of the kinetic parameters for nucleotide incorporation: Kinetic parameters (k_{cat}, K_m, and k_{cat}/K_m) for natural and non-natural nucleotides were obtained as previously described.[18] In brief, for the replication of an abasic site, assays were performed by preincubating DNA substrate (1000 nM) with variable nucleotide concentrations (0–500 μM) in the presence of Mg^{2+} (10 mM) and initiating the reaction through the addition of E *coli* Kienow fragment (12 nM). Similar conditions were employed for HIV-1 reverse transcriptase. In this case, assays were performed by preincubating DNA substrates (500 nM) with variable nucleotide concentrations (0–500 μM) in the presence of Mg^{2+} (10 mM). Polymerization reactions were initiated by adding HIV-1 reverse transcriptase (50 nM). Slight modifications to these reaction conditions were used to measure nucleotide incorporation opposite an unmodified thymine. In this case, assays used Kienow fragment (60 nM) and 13/20T-mer DNA substrate (1000 nM) with variable nucleotide concentrations (0–500 μM).

Steady-state rates were obtained from the linear portion of the time course and were fit to Equation (1):

$$\text{rate} = mt + b \quad (1)$$

where m is the slope of the line and the rate of polymerization reaction (nM s^{-1}), b is they-intercept, and t is time. Data for the dependency of rate as a function of nucleotide concentration were fit to the Michaelis–Menten equation (Equation (2)):

$$v = \frac{V_{max}[dXTP]}{K_m + [dXTP]} \quad (2)$$

where v is the rate of product formation (nM s^{-1}), V_{max} is the maximal rate of polymerization, K_m is the Michaelis constant for dXTP, and [dXTP] is the concentration of nucleotide substrate. The turnover number, k_{cat}, is V_{max} divided by the final concentration of polymerase used in the experiment.

Quantifying the inhibitory effects of non-natural nucleotides: The inhibitory effects of non-natural nucleotides on HIV-1 RT activity was measured using HIV-1 RT (50 nM) and duplex DNA (500 nM) containing an abasic site template (DNA_{5p}) or duplex DNA containing a thymine template (DNA_T). A small aliquot containing dATP (1.5 μM; opposite T) or dATP (100 μM; opposite 5P) and variable concentrations (0–500 μM) of non-natural nucleotide was added to initiate the polymerization reaction. Aliquots of the reaction were quenched with EDTA (200 mM, pH 7.4) at times ranging from 10–300 s, and product formation was quantified as described above. appK_i values were obtained using the x-intercept from Dixon plot analysis (1/rate versus inhibitor concentration). True inhibition constants designated as K_i values were obtained using Equation (3):

$$K_i = \frac{\text{app}K_i}{1 + ([dNTP]/K_m)} \quad (3)$$

where K_m is the Michaelis constant for dXTP, and [dNTP] is the concentration of nucleotide substrate, and appK_i is the apparent inhibition constant determined from the Dixon plot. All measured K_i values represent an average of two independent determinations.

Dead-end inhibition studies were performed by varying the concentration of dNTP substrate at several fixed concentrations of non-natural nucleotide (0–500 μM). Reciprocal velocities (1/rate) were plotted versus reciprocal dNTP concentrations (1/dNTP). All plots and replots used to define K_i values were linear. Data were fit to the following rate equations to validate the mode of inhibition and to provide K_i, and/or K_i values. Data conforming to a competitive inhibition pattern were fit to Equation (4):

$$\frac{1}{v} = \frac{K_m}{V_{max}}\left[1 + \frac{I}{K_i}\right] \times \frac{1}{[dXTP]} + \frac{1}{V_{max}} \quad (4)$$

data conforming to an uncompetitive inhibition pattern were fit to Equation (5):

$$\frac{1}{v} = \frac{K_m}{V_{max}} \times \frac{1}{[dXTP]} + \frac{1}{V_{max}}\left[1 + \frac{I}{K_i}\right] \quad (5)$$

data conforming to a noncompetitive inhibition pattern were fit to Equation (6):

$$\frac{1}{v} = \frac{K_m}{V_{max}}\left[1 + \frac{I}{K_i}\right] \times \frac{1}{[dXTP]} + \frac{1}{V_{max}}\left[1 + \frac{I}{K_i}\right] \quad (6)$$

Molecular modeling and docking: Coordinates of the crystal structures used for molecular modeling were taken from the Research Collaboratory for Structural Bioinformatics Protein Data Bank (http://www.pdb.org). Structural models for the putative Kienow DNA_{5p} dNTP ternary complex was made from the cocrystal structures of Klentaq DNA_{5p} dNTP (PDB ID: 3LWL)[15a] since only the crystal structures of the binary complexes of the Kienow fragment have been determined in complex with DNA[15b,c] or dNTP.[15d] Both enzymes are structurally and functionally homologous.[27] Conserved residues of the Kienow fragment corresponding to those in the Klentaq fragment were determined through primary sequence alignment using the BLOSUM62 substitution matrix.[28] Hydrophobicity surface models were generated using the Kyte–Doolittle[29] hydrophobicity scale provided in UCSF Chimera 1.5.3.[30]

The abasic site in HIV-1 RT DNA dNTP (PDB ID: 3KK2)[16] ternary complex was created by removing the templating nucleobase partner of the incoming dNTP in the active site and energy minimized through molecular mechanics using the Molecular Operating Environment (MOE 2010.10) modeling software (http://www.chemcomp.com).

The MOE program was used for the docking simulation studies as well as to search for favorable binding configurations between 5-PhITP and the macromolecular target, HIV-1 RT. The coordinates of the crystal structure of the macromolecular target, HIV-1 RT bound to TSAO inhibitor (PDB ID: 3Q09), were downloaded from RCSB. Prior to the docking simulation, the TSAO inhibitor was deleted and hydrogens were added to the crystal structure using the standard settings of MOE's Protonate 3D. The Site Finder application in MOE was then used to calculate possible binding sites from the three-dimensional atomic coordinates of the enzyme. Sites that include the residues of the nucleotide and hydrophobic binding pockets were selected as potential binding pocket by populating them with "dummy atoms" in preparation for the docking simulations with 5-PhITP. MOE-dock generated a maximum of 1000 poses with the Triangle Matcher feature, and the best 30 poses were retained for further relaxation and scored based on the Affinity dG scoring function of MOE. The best scoring pose was subjected for further relaxation and forcefield refinements.

Abbreviations

EDTA: ethylenediaminetetraacetate sodium salt; dNTP: deoxynucleoside triphosphate; T: thymine; dAMP: adenosine-2'-deoxyriboside monophosphate; dATP: adenosine-2'-deoxyriboside triphosphate; dGTP: guanine-2'-deoxyriboside triphosphate; dTIP: thymine-2'-deoxyriboside triphosphate; 5-NITP: 5-nitroindolyl-2'-deoxynucleoside triphosphate; 5-CITP: 5-carboxylindolyl-2'-deoxynucleoside triphosphate; 5-MeCITP: 5-methylcarboxylindolyl-2'-deoxynucleoside triphosphate; 5-PhlTP: 5-phenylindolyl-2'-deoxynucleoside triphosphate; 5-FS-PhlTP: 5-pentafluorophenylindolyl-2'-deoxynucleoside triphosphate; 5-F40Me-PhlTP: 5-tetrafluoro-4-methoxy-phenylindolyl-2'-deoxynucleoside triphosphate; lndTP: indolyl-2'-deoxynucleoside triphosphate; 5-CHITP: 5-cyclohexyl-2'-deoxynucleoside triphosphate.

Acknowledgements

This research was funded by the National Institutes of Health (CAI 18408 to A.J.B.).

Keywords: desolvation energies • DNA polymerase • mutagenesis • non-natural nucleotides • translesion DNA synthesis

[IJ a) T. A. Steitz, *J. Biol. Chem.* **1999,** *274,* 17395 17398; b) C. M Joyce, 5. J. Benkovic, *Biochemistry* **2004,** *43,* 14317 14324; c) C. Castro, E Smidansky, K R Maksimchuk, J. J. Arnold, *V.* 5. Korneeva, M Giitte, W. Konigsberg, C. E Cameron, *Proc. Not/. Acad. Sci. USA* **2007,** *104,* 4267 4272.

[2J C. lndiani, L D. Langston, 0. Yurieva, M F. Goodman, M O'Donnell, *Proc. Natl. Acad. Sci. USA* **2009,** *106,* 6031 6038.

[3J J. Beckman, K Kincaid, M Hocek, T. Spratt, J. Engels, R Cosstick, R D. Kuchta, *Biochemistry* **2007,** *46,* 448 460.

[4J P. Cuniasse, G. *V.* Fazakerley, W. Guschlbauer, B. E Kaplan, L C. Sowers, *J. Mo/. Biol.* **1990,** 273, 303 314.

[SJ a) T. J. Matray, E.T. Kool, *Nature* **1999,** *399,* 704 708; b) E.T. Kool, *Annu. Rev. Biochem.* **2002,** 77, 191 219.

[6J a) 5. Moran, R X. Ren, E.T. Kool, *Proc. Natl. Acad. Sci. USA* **1997,** *94,* 10506 10511; b) I Hirao, T. Mitsui, M Kimoto, 5. Yokoyama, *J. Am. Chem. Soc.* **2007,** *729,* 15549 15555; c) Y. Hari, G. T. Hwang, A. M Leconte, N. Joubert, M Hocek, F. E Romesberg, *ChemBioChem* **2008,** *9,* 2796 2799; d) G. T. Hwang, F. E Romesberg, *J. Am. Chem. Soc.* **2008,** *130,* 14872 14882; e) G. Stengel, B. W. Purse, L M Wilhelmsson, M Urban, R D. Kuchta, *Biochemistry* **2009,** *48,* 7547 7555; f) M Chiaramonte, C. L. Moore, K Kincaid, R D. Kuchta, *Biochemistry* **2003,** *42,* 10472 10481.

[7J a)X. Zhang, I Lee, A.J. Berdis, *Org. Biomol. Chem.* **2004,** 2, 1703 1711; b) X. Zhang, I Lee, X. Zhou, A J. Berdis, *J. Am. Chem. Soc.* **2006,** 728, 143 149; c) X. Zhang, A. Donnelly, I Lee, A J. Berdis, *Biochemistry* **2006,** *45,* 13293 13303; d) D. Vineyard, X. Zhang, A. Donnelly, I Lee, A J. Berdis, *Org. Biomol. Chem.* **2007,** 5, 3623 3630.

[8J E Motea, I Lee, A J. Berdis, *Nucleic Acids Res.* **2011,** *39,* 1623 1637.

[9J L K Clayton, M F. Goodman, E.W. Branscomb, D. J. Galas, *J. Biol. Chem.* **1979,** *254,* 1902 1912.

[1 OJ a) A Sheriff, E Motea, I Lee, A J. Berdis, *Biochemistry* **2008,** *47,* 8527 8537; b) M Takeshita, C. N. Chang, F. Johnson, 5. Will, A. P. Grollman, *J. Biol. Chem.* **1987,** 262, 10171 10179; c) B. Sharma, E Crespan, G. Villani, G. Maga, *Proteins Struct. Funct. Bioinf.* **2008,** 77, 715 727.

[11 J X. Zhang, I Lee, A J. Berdis, *Biochemistry* **2005,** *44,* 13101 13110.

[12J J. C. Biffinger, H. W. Kim, 5. G. DiMagno, *ChemBioChem* **2004,** 5, 622 627.

[13J H. C. Cheng, *J. Pharmaco/. Toxicol. Methods* **2001,** *46,* 61 71.

[14J W.W. Cleland, *Adv. Enzymol. Re/at. Areas Mo/. Biol.* **1967,** *29,* 1 32.

[1 SJ a) 5. Obeid, N Blatter, R Kranaster, A. Schnur, K Diederichs, W. Welte, A. Marx, *EMBO J.* **2010,** *29,* 1738 1747; b) L 5. Beese, *V.* Derbyshire, T. A. Steitz, *Science* **1993,** *260,* 352 355; c) M Teplova, 5. T. Wallace, *V.* Tereshko, G. Minasov, A M Symons, P. D. Cook, M Manoharan, M Egli, *Proc. Natl. Acad. Sci. USA* **1999,** *96,* 14240 14245; d) L 5. Beese, J. M Friedman, T. A. Steitz, *Biochemistry* **1993,** *32,* 14095 14101.

[16J E B. Lansden, D. Samuel, L Lagpacan, K M Brendza, K L White, M Hung, X. Liu, C. G. Boojamra, R L Mackman, T. Cihlar, A. 5. Ray, M E McGrath, 5. Swaminathan, *J. Mo/. Biol.* **2010,** *397,* 967 978.

[17J a) A P. Silverman, 5. J. Garforth, *V.* R Prasad, E.T. Kool, *Biochemistry* **2008,** *47,* 4800 4807; b) J. C. Morales, E.T. Kool, *Biochemistry* **2000,** *39,* 12979 12988.

[18J a) A J. Berdis, *Biochemistry* **2001,** *40,* 7180 7191; b) E Z. Reineks, A. J. Berdis, *Biochemistry* **2004,** *43,* 393 404.

[19J 5. Obeid, W. Welte, K Diederichs, A. Marx, *J. Biol. Chem.* **2012,** *287,* 14099 14108.

[20J K E Zahn, H. Belrhali, 5. 5. Wallace, 5. Doublie, *Biochemistry* **2007,** *46,* 10551 10561.

[21J K Das, J. D. Bauman, A 5. Rim, C. Dharia, A. D. Clark, Jr., M J. Camarasa, J. Balzarini, E Arnold, *J. Med. Chem.* **2011,** *54,* 2727 2737.

[22J G. Maga, D. Ubiali, R Salvetti, M Pregnolato, 5. Spadari, *Antimicrob. Agents Chemother.* **2000,** *44,* 1186 1194.

[23J N. Gianotti, A. Lazzarin, *New Microbiol.* **2005,** *28,* 281 297.

[24J A Basavapathruni, C. M Bailey, K 5. Anderson, *J. Biol. Chem.* **2004,** *279,* 6221 6224.

[25J I. Jimenez Naeher, E Alvarez, J. Morello, 5. Rodriguez Novoa, 5. de Andres, *V.* Soriano, *Expert Opin. Drug Metab. Toxicol.* **2011,** 7,457 477.

[26J C. M Joyce, *V.* Derbyshire, *Methods Enzymol.* **1995,** 262, 3 13.

[27J 5. Korolev, M Nayal, W. M Barnes, E Di Cera, G. Waksman, *Proc. Natl. Acad. Sci. USA* **1995,** *92,* 9264 9268.

[28J 5. Henikoff, J. G. Henikoff, *Proc. Not/. Acad. Sci. USA* **1992,** *89,* 10915 10919.

[29J J. Kyte, R F. Doolittle, *J. Mo/. Biol.* **1982,** 757, 105 132.

[30J E F. Pettersen, T. D. Goddard, C. C. Huang, G. 5. Couch, D. M Greenblatt, E C. Meng, T. E Ferrin, *J. Comput. Chem.* **2004,** 25, 1605 1612.